Current Applied Science and Technology e-ISSN: 2586-9396

Curr. Appl. Sci. Technol. ….., Vol... (No...), e0272364

Research article

Morpho-Physiological Responses, Growth Dynamics, and Nutrient Homeostasis of Khao Wong Kalasin Glutinous Rice (*Oryza sativa* L.) Under Stepwise Salinity Stress and Recovery

Prasit Khunsanit *, Phichaiphusit Bubparn, Tanaphoom Boonmee, Nattapon Kan-a-roon, Urai Kollboon and Keeravit Petjul

Department of Interdisciplinary Agriculture, Faculty of Agricultural Technology, Kalasin University, Kalasin, Thailand

Received: 31 May 2026, Revised: 8 September 2026, Accepted:17 September 2026, Published: 20 November 2026

Abstract

Soil salinity is a major constraint limiting rice productivity, particularly in northeastern Thailand. This study investigated morpho-physiological responses, logistic growth dynamics, and nutrient homeostasis of the glutinous rice landrace Khao Wong Kalasin (KW) and the improved cultivar RD6 under stepwise NaCl stress and post-stress recovery. Rice seedlings were exposed to 100, 200, and 300 mM NaCl under hydroponic greenhouse conditions, followed by a 7-day recovery period in salt-free nutrient solution. Salinity significantly reduced biomass accumulation, relative water content (RWC), cell membrane stability (CMS), chlorophyll content, and tiller production in both cultivars. Logistic growth analysis revealed severe suppression of biomass accumulation, with predicted asymptotic dry mass (Md_m) declining from >20 g plant^{-1} under non-stress conditions to 0.720 and 0.449 g plant^{-1} in KW and RD6, respectively. Although RD6 had a higher intrinsic growth-rate parameter (α), both cultivars showed similarly low maximum growth rates under salinity. RD6 maintained higher RWC, CMS, and chlorophyll contents during salt exposure, whereas KW showed greater chlorophyll recovery and lower residual salt injury after salt removal. Nutrient analysis in KW revealed severe ionic imbalance, characterized by excessive Na accumulation, depletion of K, Ca, S, B, Cu, Zn, Mn, and Fe, increased Na/K ratio, and reduced K/Mg ratio. Overall, RD6 maintained physiological function more effectively during salinity, whereas KW exhibited superior post-stress recovery. These findings provide useful insights into cultivar-specific salinity responses and recovery in rice.

Keywords: biomass; cell membrane stability; salt stress; Khao Wong Kalasin sticky rice; logistic function; nutrient accumulation; stress recovery

*Corresponding author: E-mail: prasit.kh@ksu.ac.th
https://doi.org/10.55003/cast.2026.272364
Copyright © 2026 by King Mongkut's Institute of Technology Ladkrabang, Thailand. This is an open access article under the CC BY-NC-ND license (http://creativecommons.org/licenses/by-nc-nd/4.0/).

1. Introduction

Soil salinity is among the most damaging abiotic stresses affecting rice production worldwide, with salt-affected soils estimated to impair crop growth on approximately 20% of irrigated agricultural land (Munns et al., 2020; Tarolli et al., 2024). In northeastern Thailand, salinity is a long-standing constraint caused by saline parent materials, shallow groundwater, and seasonal evapotranspiration that promotes capillary salt rise, threatening the sustainability of lowland rice production (Arunin & Pongwichian, 2015; Vanavichit et al., 2018). Rice is moderately salt-sensitive, with substantial growth inhibition occurring above 3–4 dS m^{-1} and progressively greater physiological disruption under severe salinity (Liu et al., 2022; Saleem et al., 2025).

Salinity causes both osmotic and ionic stress. The initial osmotic phase restricts water uptake and cell expansion, whereas subsequent Na^+ and Cl^- accumulation disrupts photosynthesis, enzyme activity, membrane stability, and nutrient balance (Balasubramaniam et al., 2023; Liu et al., 2022). Consequently, maintenance of K^+/Na^+ homeostasis, membrane integrity, plant water status, and chlorophyll content are widely recognized indicators of salt tolerance in rice (Barman et al., 2025; Xu et al., 2024). However, these traits are usually evaluated under static stress conditions, whereas physiological recovery following stress removal remains comparatively understudied despite its importance in naturally fluctuating saline environments.

Growth modeling provides additional insight into plant responses by quantifying biomass accumulation over time. Logistic growth models describe biomass accumulation using two biologically meaningful parameters: the asymptotic maximum biomass (Md_m) and the growth rate constant (α), allowing assessment of both the extent and temporal progression of growth inhibition (Hunt, 1982; Thornley & Johnson, 1990). Although logistic models have been applied to rice plant height and horticultural seedling growth (Hsieh et al., 2021; Hsieh et al., 2026), they have not been used to characterize biomass dynamics under progressive salinity stress in rice landraces.

Nutrient homeostasis represents another important component of salt tolerance. Salinity reduces the uptake of essential macro- and micronutrients through ionic competition while promoting Na^+ accumulation, leading to altered nutrient partitioning between shoots and roots (Akter & Oue, 2018; Sackey et al., 2025). Nevertheless, comprehensive organ-specific ionomic analyses under progressive high-salinity stress remain scarce, particularly for traditional Asian rice landraces.

Khao Wong Kalasin sticky rice (KW) is a traditional glutinous landrace cultivated in Kalasin Province, northeastern Thailand, where saline soils are widespread. Despite its agronomic and cultural importance, its physiological responses to salinity, particularly its capacity for post-stress recovery, remain unknown. Therefore, this study aimed to (i) characterize the morphophysiological responses of KW and the improved cultivar RD6 under stepwise NaCl stress (100-300 mM) and subsequent recovery; (ii) apply logistic growth modeling to quantify biomass accumulation dynamics and identify cultivar-specific growth responses; and (iii) determine the shoot and root ionomic profiles of KW to elucidate nutrient partitioning under severe salinity.

2. Materials and Methods

2.1 Plant material and experimental design

The experiment was conducted under greenhouse conditions at Kalasin University (Kalasin Province, Thailand) from January to April 2026. Two *Oryza sativa* L. cultivars were evaluated: Khao Wong Kalasin sticky rice (KW), a traditional glutinous landrace sourced from local farmers in Khao Wong District, and RD6, a commercial glutinous cultivar used as a reference. The experiment was arranged as a completely randomized design (CRD) with two treatments (non-stress and salt stress), two cultivars, and four replications per treatment-by-cultivar combination.

Seeds were germinated in water for 14 days, then transplanted individually into 20 cm^3 hydroponic trays supported by sponge holders and cultivated in AB mix nutrient solution for 21 days (Balansag et al., 2023). Nutrient Solution A comprised calcium nitrate ($Ca(NO_3)_2$, 115 g L^{-1}), Fe-EDTA (4 g L^{-1}), Fe-EDDHA (2 g L^{-1}), and boric acid (H_3BO_3, 1 g L^{-1}). Solution B contained potassium nitrate (KNO_3, 100 g L^{-1}), magnesium sulfate ($MgSO_4$, 50 g L^{-1}), monopotassium phosphate (KH_2PO_4, 27 g L^{-1}), monoammonium phosphate ($NH_4H_2PO_4$, 5 g L^{-1}), and chelated micronutrients (Cu-EDTA, Mn-EDTA, Zn-EDTA at 1 g L^{-1} each) plus a trace element blend. Working solutions were prepared by diluting 20 mL of each stock solution into 10 L of groundwater (EC ≈ 0.15 dS m^{-1}), yielding a final nutrient solution EC of approximately 0.52 dS m^{-1}.

2.2 Salt stress and recovery protocol

After establishment, plants assigned to the salt-stress treatment were exposed to NaCl in the AB nutrient solution using a stepwise salinity regime. The NaCl concentration was increased sequentially from 100 mM (EC ≈ 12.8 dS m^{-1}; days 1–3), representing moderate salinity stress, to 200 mM (EC ≈ 16.2 dS m^{-1}; days 4–7), representing severe salinity stress, and finally to 300 mM (EC ≈ 20.4 dS m^{-1}; days 8–10), representing extreme salinity stress. The stepwise salinity regime was adopted to progressively increase salt stress while minimizing osmotic shock associated with abrupt exposure to high NaCl concentrations. Although the maximum salinity level (300 mM NaCl; EC ≈ 20.4 dS m^{-1}) exceeds that typically encountered in most lowland rice fields, it was included to evaluate cultivar tolerance limits and post-stress recovery under controlled experimental conditions. Solutions were renewed at each concentration step to maintain consistent salinity and nutrient composition. Following the stress period, plants were thoroughly rinsed with distilled water and transferred to fresh AB mix nutrient solution for a 7-day recovery phase (days 11–17). Non-stress control plants were maintained continuously in AB mix nutrient solution (EC ≈ 0.52 dS m^{-1}).

2.3 Morphological parameters

Tiller number (TN) was assessed by direct counting of active tillers at each measurement point (days 0, 3, 7, 10, and 17). Salt injury score (SIS) was evaluated visually using the standard 1-9 scale described by Gregoria et al. (1997), where 1 indicates no visible injury and 9 indicates plant death.

2.4 Biomass accumulation and allocation

Plants were separated into shoot (S) and root (R) fractions at each harvest. Fresh mass (Mf) was recorded immediately. Samples were oven-dried at 70°C to constant weight to determine dry mass (Md). The shoot dry-to-fresh mass ratio (S_Md/Mf) was calculated as a dehydration index. The root-to-shoot dry mass ratio (Md_R/S) was computed to assess salt-induced biomass partitioning shifts.

2.5 Logistic growth modeling

Total plant dry mass (shoot + root) over time was described using the three-parameter logistic growth function (Hunt, 1982; Thornley & Johnson, 1990):

$$Md = \frac{Md_0 Md_m}{Md_0 + (Md_m - Md_0)e^{-\alpha t}}$$

where Md(t) is total plant dry mass (g plant^{-1}) at time t (days), Md_0 is the initial dry mass, Md_m is the asymptotic maximum dry mass, and α is the intrinsic growth rate constant (day^{-1}). The instantaneous growth rate was derived as:

$$\frac{dMd}{dt} = \frac{mn\alpha e^{-\alpha t}}{(Md_0 + ne^{-\alpha t})^2}$$

where $m = Md_m \times Md_0$ and $n = Md_m - Md_0$. Parameters were estimated by nonlinear least-squares regression using the *nls()* function in R (R Core Team, 2023), with starting values derived from observed minimum and maximum biomass data. Data from the recovery stage (day 17) were excluded from model fitting under the salt-stress treatment to avoid confounding growth resumption with stress-phase kinetics.

2.6 Leaf water status and membrane integrity

Relative water content (RWC) was determined on 4-cm segments of the youngest fully expanded leaf: fresh mass (Mf) was recorded immediately after excision; samples were then rehydrated in deionized water for 4 h to obtain turgid mass (Mtg); and oven-dried at 70°C to constant weight to determine dry mass (Md). RWC (%) was calculated as [(Mf − Md) / (Mtg − Md)] × 100.

Cell membrane stability (CMS) was assessed by electrolyte leakage. Approximately 15 mg of leaf tissue was cut into 0.2-cm pieces, incubated in deionized water (EC ≈ 0.005 dS m^{-1}) at 25°C for 4 h, and initial conductivity (EC_0) recorded. Samples were subsequently heated at 100°C for 30 min, cooled to 25°C, and final conductivity (EC_1) measured. CMS (%) was calculated as [1 − (EC_0 / EC_1)] × 100.

2.7 Chlorophyll content

Chlorophyll was extracted from leaf disc samples (0.283 cm^2) in undiluted N,N-dimethylformamide (DMF) at 25°C for 5 days until complete chlorosis (Moran, 1982). Absorbance at 647 and 664 nm was measured spectrophotometrically. Chlorophyll fractions (g m^{-2}) were calculated as:

$$\text{Chl } a = [(-2.99 \times A647) + (12.64 \times A664)] \times Vol / (D \times Area \times 100)$$

$$\text{Chl } b = [(23.26 \times A647) - (5.60 \times A664)] \times Vol / (D \times Area \times 100)$$

$$\text{Chl } total = [(20.27 \times A647) + (7.04 \times A664)] \times Vol / (D \times Area \times 100)$$

where Vol is the extraction volume (mL), Area is the leaf disc area (cm^2), and D is the dilution factor (set to 1 for undiluted extracts).

2.8 Nutrient analysis

Shoot and root dry tissue samples from KW (300 mM NaCl, day 10) were dried at 70°C for 3 days and ground into a fine powder. Total nitrogen (N) was determined separately using the micro-Kjeldahl method. For the determination of the remaining elements, the ground samples were ashed at 550°C for 5 h, and the resulting ash was dissolved in 10 mL of 1 N HCl and diluted with 10 mL of distilled water. The concentrations of six macronutrients (P, K, S, Ca, Mg, and Na) and six micronutrients (B, Cu, Zn, Mn, Mo, and Fe) were determined by inductively coupled plasma optical emission spectrometry (ICP-OES) following (Poovarodom, 2009). Macronutrient contents (mg $plant^{-1}$) were calculated by multiplying nutrient concentration (% dry mass) by organ dry mass and converting to mg. Micronutrient contents (mg $plant^{-1}$) were calculated by multiplying nutrient concentration (μg g^{-1} dry mass) by organ dry mass and converting μg to mg.

2.9 Statistical analysis

Statistical analyses were performed using R 4.3.1 (R Core Team, 2023) in RStudio (Posit Team, 2026). Three-way analysis of variance (ANOVA) was used to evaluate the effects of treatment, cultivar, day, and their interactions. Mean comparisons were conducted using Tukey's honestly significant difference (HSD) test at $P \leq 0.05$. Uncertainty in the logistic model parameters was assessed using bootstrap confidence intervals. Graphs were generated using the *ggplot2* package (Wickham, 2009).

Pearson correlation coefficients were calculated separately for KW and RD6 to assess relationships among morpho-physiological traits during the salinity stress and recovery period (days 0-17), excluding the control treatment. Differences in correlation strength between cultivars were tested using Fisher's *r*-to-*z* transformation (Fisher, 1915). P-values from multiple correlation comparisons were adjusted using the Benjamini–Hochberg false discovery rate (FDR) method, with FDR-adjusted $P<0.05$ considered statistically significant (Benjamini & Hochberg, 1995).

3. Results and Discussion

3.1 Results

Three-way ANOVA revealed significant main effects of treatment on most measured traits, whereas significant cultivar effects were detected only for tiller number, shoot dry mass, root dry mass, shoot dry/fresh mass ratio, and root/shoot dry mass ratio (Table 1). Sampling day significantly affected most growth and physiological parameters. Significant treatment × day interactions were observed for nearly all growth-related traits, indicating

that the effects of salinity varied over time. In contrast, treatment × cultivar interactions were significant only for root dry mass and shoot dry/fresh mass ratio, whereas significant three-way interactions were detected only for shoot dry/fresh mass ratio and chlorophyll-related traits.

Table 1. Summary of three-way ANOVA for the measured parameters under non-stress and salt stress.

Parameter	Treatment	Cultivar	Day	Treatment × Cultivar	Treatment × Day	Cultivar × Day	Treatment × Cultivar × Day
TN	***	***	***	ns	***	ns	ns
SIS	***	ns	***	ns	***	ns	ns
MdS	***	***	***	ns	***	ns	ns
MdR	***	***	***	*	***	*	ns
S_Md/Mf	***	***	***	**	***	ns	**
Md_R/S	***	*	***	ns	***	ns	ns
RWC	***	ns	**	ns	*	*	ns
CMS	***	ns	***	ns	***	ns	ns
Chl *a*	***	ns	ns	ns	**	**	**
Chl *b*	ns	ns	ns	ns	ns	ns	ns
Chl *total*	ns	ns	ns	ns	*	*	**
Chl *a/b*	*	ns	ns	ns	ns	ns	ns

TN, tiller number; SIS, salt injury score; MdS, shoot dry mass; MdR, root dry mass; S_Md/Mf, shoot dry-to-fresh mass ratio; Md_R/S, root-to-shoot dry mass ratio; RWC, relative water content; CMS, cell membrane stability; Chl *a*, chlorophyll *a*; Chl *b*, chlorophyll *b*; Chl *total*, total chlorophyll; Chl *a/b*, chlorophyll *a/b* ratio.
*, **, and *** indicate significance at $p \leq 0.05$, $p \leq 0.01$, and $p \leq 0.001$, respectively; ns = not significant.

3.1.1 Tiller development and salt injury progression

Under non-stress conditions, tiller number (TN) increased progressively in both cultivars, reaching approximately 18 and 14 tillers plant^{-1} in KW and RD6, respectively, at day 17. KW produced significantly more tillers than RD6 at days 7 and 17, whereas no significant differences were detected at the other sampling dates. Salt stress markedly inhibited tiller development in both cultivars, and no significant differences in TN were observed between cultivars throughout the stress period (Figure 1A).

Salt injury score (SIS) remained at the minimum value of 1 under non-stress conditions. Under salt stress, SIS increased progressively in both cultivars with increasing NaCl concentration. No significant differences between cultivars were detected during the stress period; however, RD6 exhibited a significantly higher SIS than KW after recovery (day 17), indicating greater residual salt injury (Figure 1B).

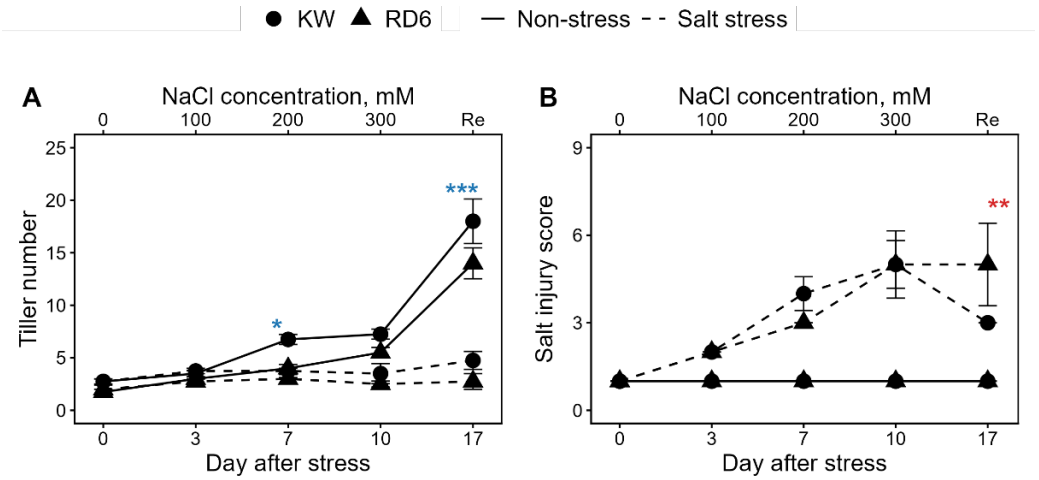


Figure 1. A) Tiller number (TN) and B) salt injury score (SIS) of KW and RD6 under non-stress and salt stress conditions. Values are presented as means ± SE (n = 4). Re, recovery. Blue and red asterisks indicate significant differences between cultivars within the non-stress and salt stress treatments, respectively, based on Tukey-adjusted pairwise comparisons (*$p \leq 0.05$, **$p \leq 0.01$, ***$p \leq 0.001$).

3.1.2 Biomass accumulation and partitioning

Under non-stress conditions, shoot and root dry mass increased progressively in both cultivars throughout the experimental period. KW accumulated greater shoot and root dry mass than RD6, reaching approximately 4.7 and 1.4 g plant^{-1}, respectively, at day 17. Pairwise comparisons indicated that shoot and root dry mass were significantly higher in KW than in RD6 at day 17, whereas no significant differences were detected at earlier sampling dates. Salt stress markedly suppressed biomass accumulation in both cultivars, reducing shoot and root dry mass throughout the stress period. Although biomass increased after salt removal, no significant differences between cultivars were observed under salt stress (Figure 2A,B).

The shoot dry mass-to-fresh mass ratio (S_Md/Mf), an indicator of tissue dehydration, with higher values indicating greater water loss, increased under salt stress, reaching approximately 29-30% at 300 mM NaCl in both cultivars (Figure 2C). Under non-stress conditions, RD6 exhibited a significantly higher S_Md/Mf than KW from days 0 to 10, whereas no cultivar difference was detected after recovery. Under salt stress, cultivar differences were observed only at days 0 and 17, with RD6 exhibiting a higher S_Md/Mf after recovery.

The root-to-shoot dry mass ratio (Md_R/S), an indicator of biomass allocation between roots and shoots in which higher values reflect greater allocation to roots, remained relatively stable under non-stress conditions but declined under severe salt stress before increasing during the recovery phase (Figure 2D). No significant differences between cultivars were detected under non-stress conditions. Under salt stress, however, RD6 exhibited a significantly higher Md_R/S than KW after recovery, suggesting relatively greater biomass allocation to roots, whereas no significant cultivar differences were observed during the stress period.

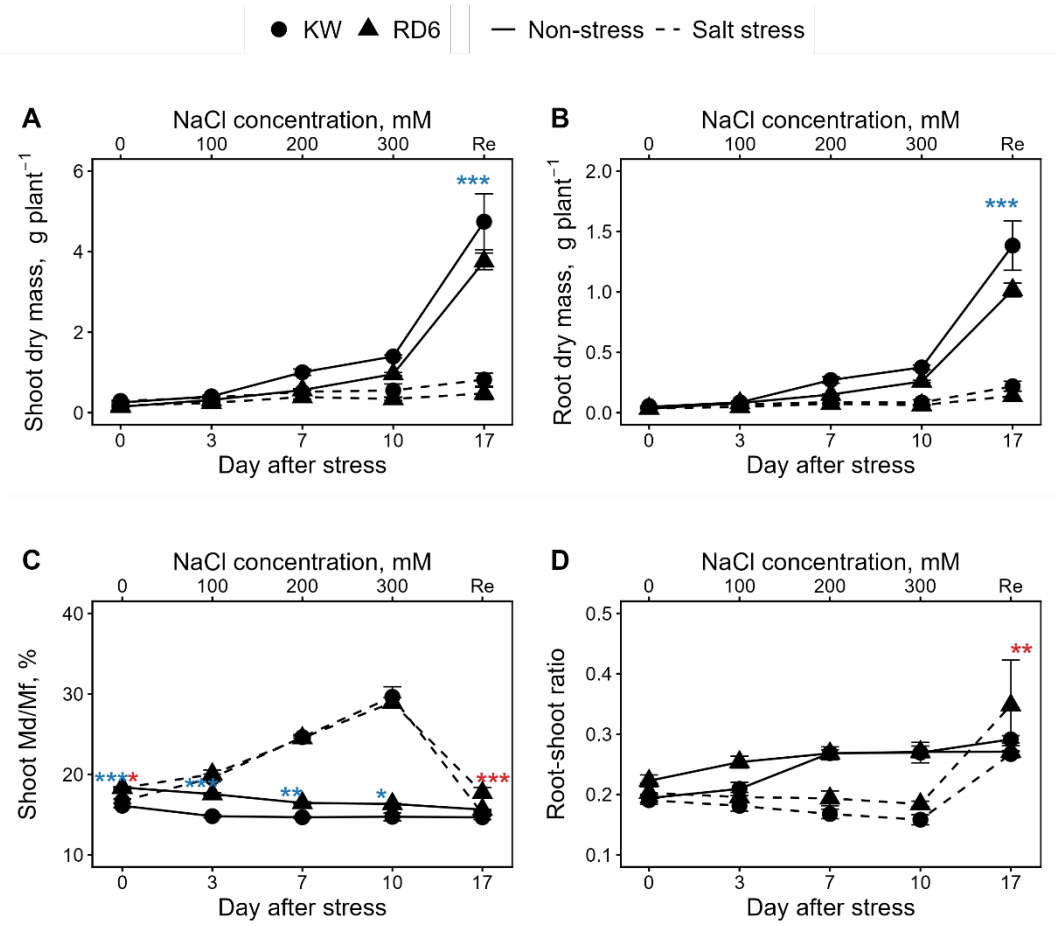


Figure 2. A) Shoot dry mass, B) root dry mass, C) shoot dry mass to fresh mass and D) root-shoot dry mass ratio of KW and RD6 under non-stress and salt stress conditions. Values are presented as means ± SE (n = 4). Re, recovery. Blue and red asterisks indicate significant differences between cultivars within the non-stress and salt stress treatments, respectively, based on Tukey-adjusted pairwise comparisons (*$p \leq 0.05$, **$p \leq 0.01$, ***$p \leq 0.001$).

3.1.3 Logistic growth kinetics

The logistic model adequately described total dry mass accumulation under both non-stress and salt-stress conditions, as indicated by high coefficients of determination (R^2 = 0.883-0.999) and low RMSE values (0.014-0.131 g plant^{-1}) (Table 2; Figure 3A). Under non-stress conditions, the estimated asymptotic dry mass (Md_m) reached the upper parameter bound (>20 g plant^{-1}) in both cultivars, indicating that biomass accumulation had not reached an asymptotic plateau by the end of the experimental period. The intrinsic growth-rate parameter (α) was similar between cultivars, with values of 0.206 and 0.216 day^{-1} for KW and RD6, respectively. The maximum growth rates (dMd/dt) were 0.872 and 0.785 g plant^{-1} day^{-1} for KW and RD6, respectively, with both occurring at day 17 (Table 2; Figure 3B).

Table 2. Logistic growth model parameters and goodness-of-fit statistics for total dry mass accumulation in KW and RD6 rice under salinity stress

Treatment	Cultivar	Md_0 (g plant^{-1})	Md_m (g plant^{-1})	α (day^{-1})	Max dMd/dt (g plant^{-1} day^{-1})	Day at max dMd/dt	R^2	RMSE
Non-stress	KW	0.263±0.118	>20	0.206±0.064	0.872	17	0.996	0.131
	RD6	0.157±0.048	>20	0.216±0.041	0.785	17	0.999	0.056
Salt Stress	KW	0.341±0.027	0.720±0.107	0.228±0.099	0.041	0.45	0.986	0.014
	RD6	0.199±0.066	0.449±0.094	0.382±0.368	0.043	0.60	0.883	0.034

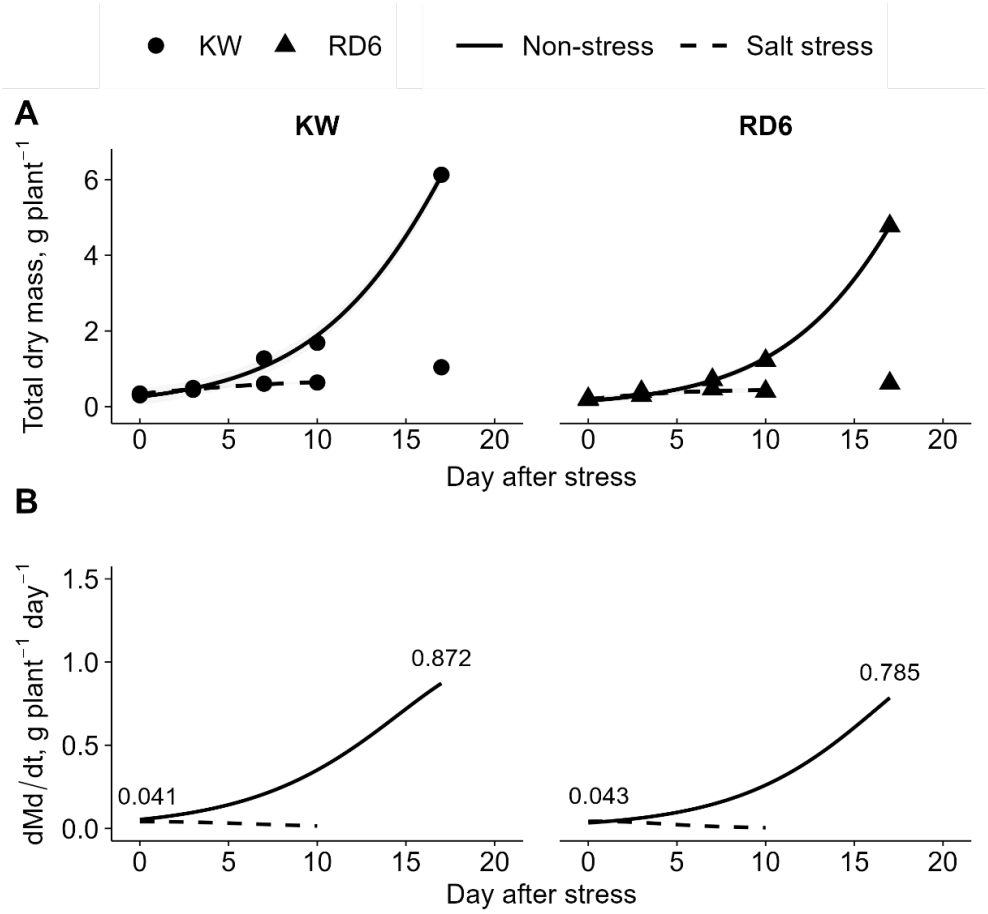


Figure 3. Total dry mass (A) and growth rate (B) of KW and RD6 under non-stress and salt stress conditions during a 17-day period. Total dry mass (g plant^{-1}) was described using a logistic function, and growth rate (dMd/dt; g plant^{-1} day^{-1}) was derived from the fitted model. Data from day 17 under salt stress were excluded due to the recovery stage. Symbols ● and ▲ represent mean±standard error, whereas solid (—) and dashed (--) lines indicate model predictions.

Salt stress markedly reduced the estimated asymptotic dry mass to 0.720 g plant^{-1} in KW and 0.449 g plant^{-1} in RD6, indicating a substantial reduction in biomass accumulation. The estimated initial dry mass (Md_0) was 0.341 and 0.199 g plant^{-1} for KW and RD6, respectively, whereas the intrinsic growth-rate parameter (α) increased to 0.228 day^{-1} in KW and 0.382 day^{-1} in RD6. Despite the higher estimated α in RD6, both cultivars exhibited similarly low maximum growth rates under salt stress (0.041-0.043 g plant^{-1} day^{-1}). The maximum growth rate occurred within the first day after stress initiation (0.45 day in KW and 0.60 day in RD6), after which growth progressively declined toward zero with increasing salinity (Figure 3B).

3.1.4 Relative water content and cell membrane stability

Under non-stress conditions, RWC remained above 83% in both cultivars throughout the experiment (Figure 4A). Salt stress progressively decreased RWC in both cultivars, with a greater decline in KW than in RD6. At 200 and 300 mM NaCl, RWC in KW decreased to approximately 56% and 46%, respectively, whereas RD6 maintained higher values of approximately 87% and 74%. Consequently, RWC was significantly higher in RD6 than in KW at 100, 200, and 300 mM NaCl. Following recovery, RWC increased in both cultivars but remained below the corresponding non-stressed controls.

CMS remained close to 90% under non-stress conditions in both cultivars throughout the experiment. Salt stress markedly reduced CMS, particularly in KW. At 200 and 300 mM NaCl, CMS declined to approximately 40% and 28% in KW, compared with 71% and 39% in RD6. CMS was significantly higher in RD6 than in KW at 100 and 200 mM NaCl, whereas no significant cultivar difference was detected after recovery (Figure 4B). Following salt removal, CMS recovered substantially in both cultivars and approached the values observed under non-stress conditions.

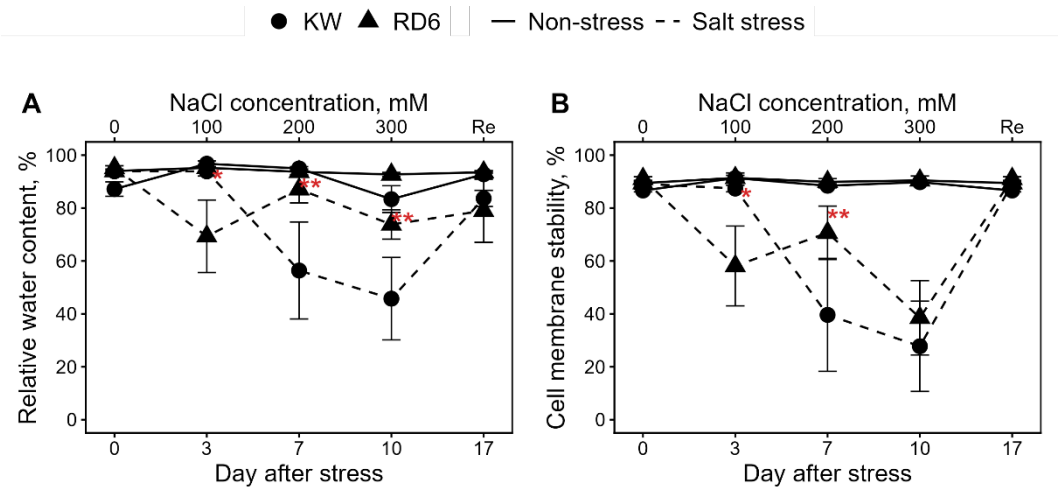


Figure 4. A) Relative water content (RWC) and B) cell membrane stability (CMS) of KW and RD6 under non-stress and salt stress conditions. Values are presented as means±SE (n = 4). Re, recovery. Blue and red asterisks indicate significant differences between cultivars within the non-stress and salt stress treatments, respectively, based on Tukey-adjusted pairwise comparisons (*p≤0.05, **p≤0.01, ***p≤0.001).

3.1.5 Chlorophyll responses

Under non-stress conditions, chlorophyll *a*, chlorophyll *b*, total chlorophyll, and the chlorophyll *a/b* ratio remained relatively stable in both cultivars throughout the experimental period (Figure 5). Salt stress altered chlorophyll *a* content in both cultivars, with a more pronounced reduction in KW than in RD6. In KW, chlorophyll *a* declined to approximately 0.16 g m^{-2} at 200 mM NaCl (day 7), whereas RD6 maintained values above 0.30 g m^{-2} throughout the stress period. Consequently, chlorophyll *a* was significantly higher in KW at 100 mM NaCl, higher in RD6 at 200 mM NaCl, and higher again in KW after recovery (Figure 5A). Following salt removal, chlorophyll *a* recovered to approximately the non-stressed level in KW, whereas it declined further in RD6.

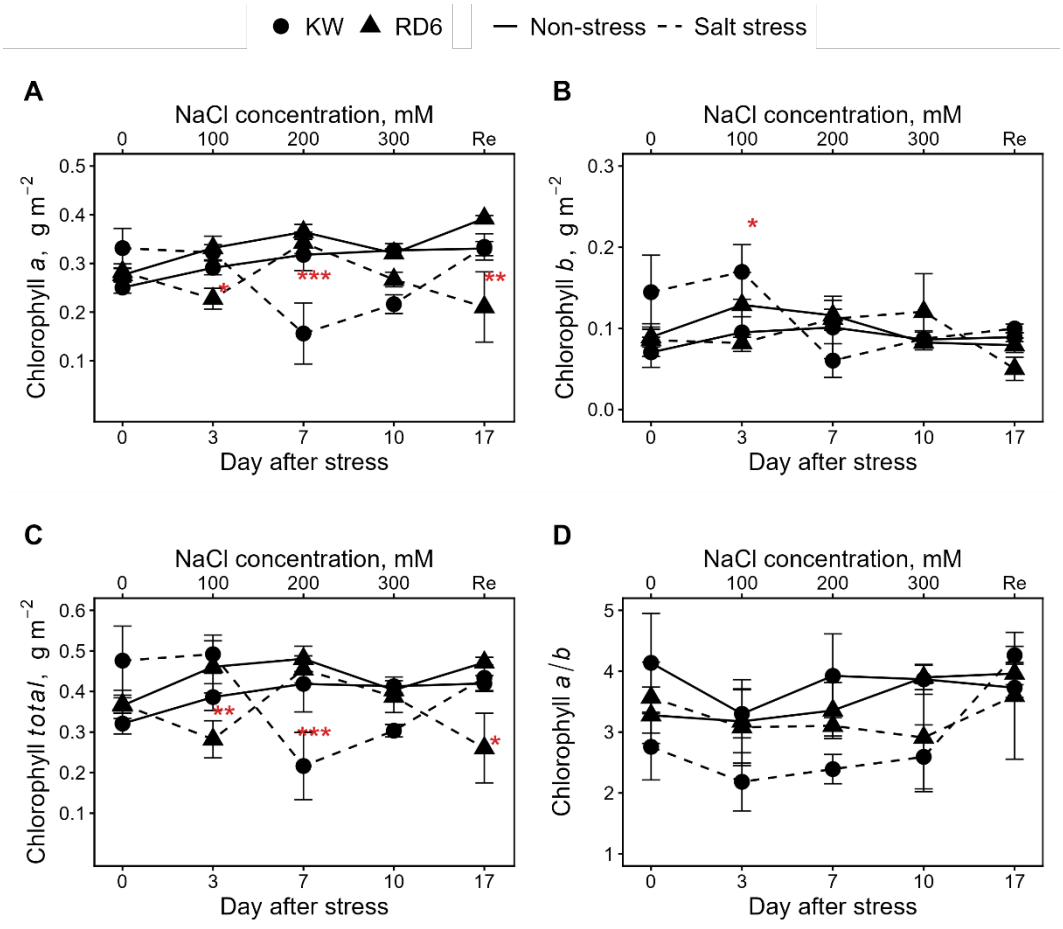


Figure 5. A) Chlorophyll *a*, B) chlorophyll *b*, C) total chlorophyll and D) chlorophyll *a/b* ratio of KW and RD6 under non-stress and salt stress conditions. Values are presented as means±SE (n = 4). Re, recovery. Blue and red asterisks indicate significant differences between cultivars within the non-stress and salt stress treatments, respectively, based on Tukey-adjusted pairwise comparisons (*$p \leq 0.05$, **$p \leq 0.01$, ***$p \leq 0.001$).

Chlorophyll *b* exhibited smaller changes than chlorophyll *a* under salt stress (Figure 5B). In KW, chlorophyll *b* increased slightly at 100 mM NaCl before decreasing at higher salinity, whereas RD6 remained relatively stable throughout the stress period. A significant cultivar difference was detected only at 100 mM NaCl, where RD6 exhibited higher chlorophyll *b* content than KW.

Total chlorophyll closely followed the pattern observed for chlorophyll *a* (Figure 5C). Significant cultivar differences were detected at 100 and 200 mM NaCl and after recovery, with KW showing higher total chlorophyll at 100 mM NaCl and after recovery, whereas RD6 was higher at 200 mM NaCl. The chlorophyll *a/b* ratio remained relatively stable in both cultivars throughout the experiment (Figure 5D). Although the ratio tended to decrease in KW under salt stress and recovered after salt removal, no significant differences between cultivars were detected at any sampling time.

3.1.6 Differential correlations among morpho-physiological traits

Pearson correlation analysis showed strong associations among several morpho-physiological traits in both KW and RD6 (Table 3). Strong positive correlations were observed for Chl *a*–Chl total, Chl *b*–Chl total, TN–MdS, TN–MdR, and MdS–MdR, while S_MdMf–CMS showed a negative correlation in both cultivars. However, most correlations did not differ significantly between cultivars. The only significant cultivar difference was observed for CMS–RWC, which was stronger in KW (r = 0.973) than in RD6 (r = 0.641).

Table 3. Differential correlations among morpho-physiological traits of KW and RD6 rice during salinity stress and recovery

Trait pair	KW r (P)	RD6 r (P)	Fisher Z	P_adj
CMS–RWC	0.973 (<0.001)	0.641 (0.002)	4.043	0.004
Chl *b*–Chl *total*	0.897 (<0.001)	0.768 (<0.001)	1.185	0.519
S_MdMf–CMS	−0.778 (<0.001)	−0.592 (0.006)	−1.049	0.595
TN–MdS	0.873 (<0.001)	0.785 (<0.001)	0.832	0.765
RWC–Chla	0.777 (<0.001)	0.630 (0.007)	0.806	0.770
TN–MdR	0.767 (<0.001)	0.642 (0.002)	0.731	0.787
Chl *a*–Chl *total*	0.959 (<0.001)	0.937 (<0.001)	0.599	0.838
MdS–MdR	0.919 (<0.001)	0.924 (<0.001)	−0.101	0.994

Values are Pearson correlation coefficients (r) with corresponding P-values in parentheses. Fisher Z represents the Z statistic for testing the difference between correlation coefficients of KW and RD6. P_adj represents P-values adjusted for multiple comparisons using the Benjamini–Hochberg false discovery rate (FDR) procedure.
TN, tiller number; SIS, salt injury score; MdS, shoot dry mass; MdR, root dry mass; SMd/Mf, shoot dry-to-fresh mass ratio; CMS, cell membrane stability; RWC, relative water content; Chl *a*, chlorophyll *a*; Chl *b*, chlorophyll *b*; Chl *total*, total chlorophyll. Significant differences between cultivars are indicated by P_adj < 0.05.

3.1.7 Nutrient accumulation and ionic homeostasis

Under non-stress conditions, KW shoots contained relatively high concentrations of K and N (Figure 6A). Salt stress significantly reduced shoot K concentration from approximately 4.7% to 3.4% dry mass and also decreased shoot S and Ca concentrations. In contrast,

shoot Mg concentration increased markedly under salinity, rising from approximately 0.17% to 3.8% dry mass. Shoot Na concentration also increased to approximately 4.0% dry mass, although the increase was not statistically significant because of high inter-replicate variation (Figure 6A). However, shoot Na content per plant increased significantly under salt stress (Figure 7C).

In roots, salt stress significantly increased both Na and Mg concentrations, reaching approximately 5.4% and 5.7% dry mass, respectively (Figure 6B). Root P concentration also increased significantly, whereas root K concentration showed a slight but non-significant decline. The Na/K ratio increased significantly in both shoots and roots under salinity, while the K/Mg ratio decreased markedly in both organs, particularly in shoots (Figure 7C,D).

At the whole-plant content level, salt stress reduced the accumulation of several macronutrients in shoots. Shoot N and K contents decreased by approximately 53% and 66%, respectively, while shoot S and Ca contents also declined significantly (Figure 7A, C). In contrast, shoot Mg and Na contents increased significantly. In roots, K content decreased significantly, whereas root Mg and Na contents increased markedly under salt stress (Figure 7B, D).

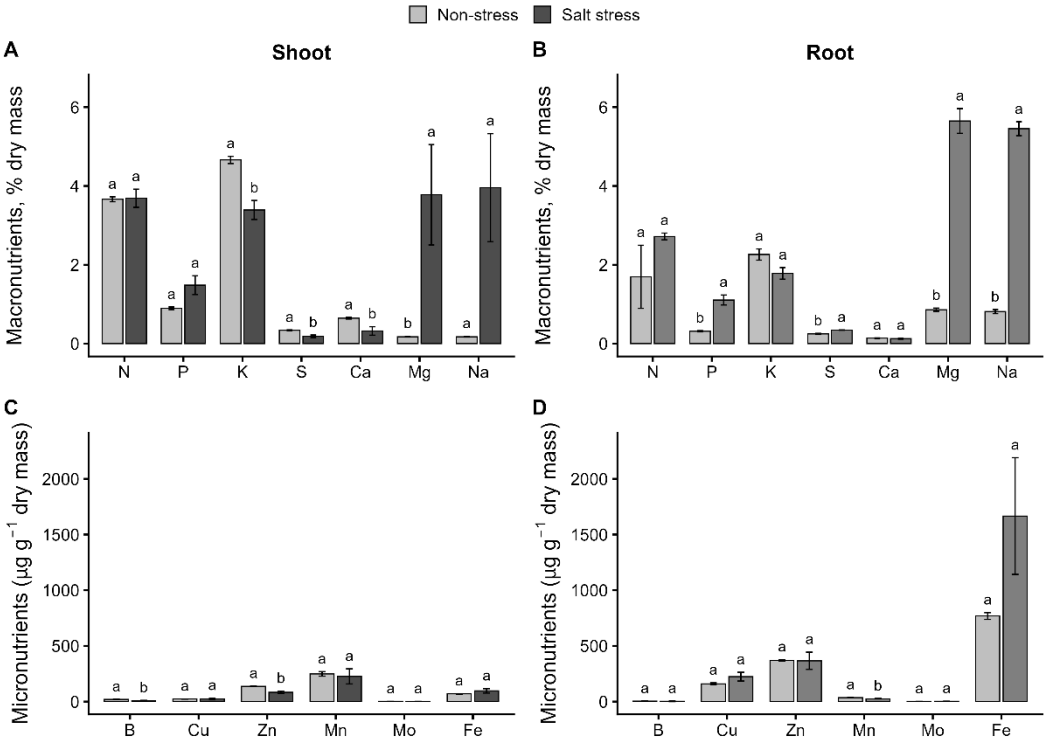


Figure 6. Nutrient concentrations in the shoots and roots of KW rice under salt stress conditions (300 mM NaCl, day 10), including macronutrients (A, B) and micronutrients (C, D). Data are presented as mean ± SE (n = 3). Different lowercase letters above the bars indicate significant differences among treatments within each nutrient according to Tukey's HSD test at $p \leq 0.05$.

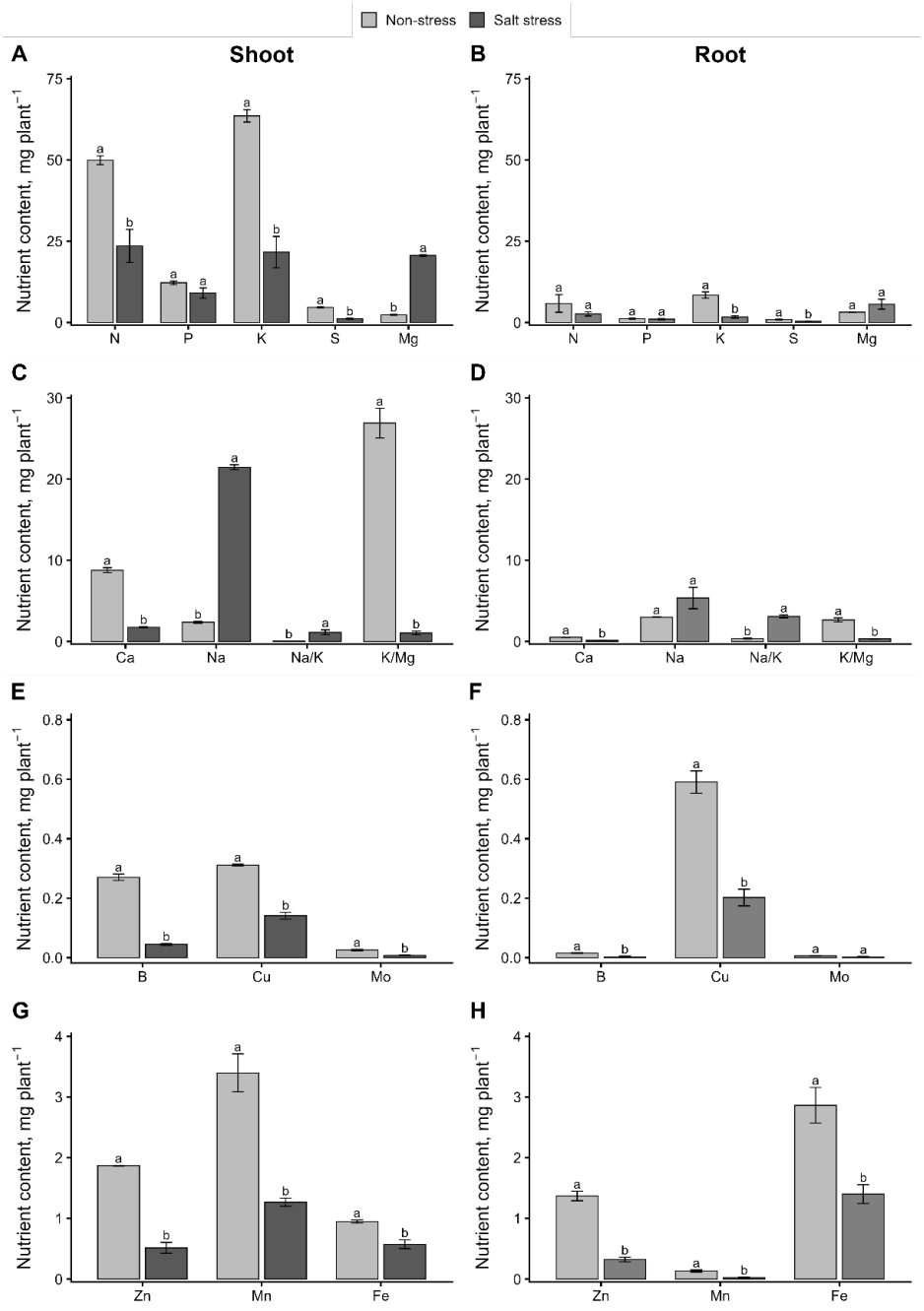


Figure 7. Nutrient contents in the shoots (A, C, E, G) and roots (B, D, F, H) of KW rice under salt stress conditions (300 mM NaCl, day 10). Data are presented as mean±SE (n = 3). Different lowercase letters above the bars indicate significant differences among treatments within each nutrient according to Tukey's HSD test at $p \leq 0.05$.

Micronutrient concentrations were also affected by salinity stress. In shoots, B and Zn concentrations decreased significantly, whereas Cu, Mn, Mo, and Fe concentrations were not significantly altered (Figure 6C). However, shoot B, Cu, Zn, Mn, and Fe contents all decreased significantly under salt stress (Figure 7E, G). In roots, Mn concentration decreased significantly, whereas root Fe concentration increased from approximately 770 to more than 1,600 μg g^{-1} dry mass under salt stress, although the increase was not statistically significant (Figure 6D). Root Fe content per plant declined significantly from approximately 2.9 to 1.4 mg $plant^{-1}$ under salinity (Figure 7H).

3.2 Discussion

Stepwise salinity markedly inhibited growth, biomass accumulation, water status, membrane stability, and chlorophyll retention in both KW and RD6, consistent with the combined osmotic and ionic effects of salt stress that impair water uptake, photosynthesis, cellular metabolism, and nutrient acquisition (Balasubramaniam et al., 2023; Liu et al., 2022). Progressive reductions in RWC, CMS, and chlorophyll under increasing NaCl concentrations indicate that physiological damage intensified as salinity increased. Although both cultivars were severely affected, they exhibited contrasting response strategies. Under non-stress conditions, KW produced greater biomass and tiller numbers than RD6. During salt exposure, however, RD6 maintained higher RWC, CMS, and chlorophyll contents, indicating greater physiological stability under stress.

Following salt removal, KW exhibited lower salt injury and greater recovery of biomass and chlorophyll than RD6, whereas RD6 showed continued chlorophyll decline despite maintaining better physiological status during the stress period. These contrasting responses suggest that salinity resilience depends not only on tolerance during stress exposure but also on the capacity to restore physiological function after stress relief, an important adaptive trait under fluctuating saline environments (Siddique et al., 2025).

The stronger CMS–RWC correlation in KW indicates a tighter association between tissue water status and membrane stability. This is consistent with Kojonna et al. (2022), who reported positive associations among RWC, CMS, and growth traits in Thai rice under salt stress. However, Santanoo et al. (2025) demonstrated that rice can maintain RWC and membrane integrity under salinity while photosynthesis, growth, and yield are substantially reduced, suggesting that maintenance of cellular water status alone may not ensure preservation of photosynthetic function. In the present study, the stronger CMS–RWC association in KW may indicate a closer coupling between tissue water status and membrane stability during salinity stress. Despite substantial physiological impairment during stress, KW showed rapid recovery of growth and chlorophyll following salt removal. This recovery capacity may be partly associated with its greater inherent growth potential, as indicated by its higher biomass accumulation and tiller production under non-stress conditions. These differences may reflect cultivar-specific regulation of growth and recovery, which was not directly investigated in this study.

The logistic model effectively characterized biomass dynamics under salinity. Salt stress markedly reduced the predicted asymptotic biomass (Md_m) and maximum growth rate in both cultivars, confirming severe inhibition of biomass accumulation. Although RD6 exhibited a higher intrinsic growth-rate parameter (α), both cultivars showed similarly low maximum growth rates under salt stress. The higher estimated α in RD6 suggests a steeper, more rapidly curtailed growth trajectory, whereas the lower α together with the slightly higher Md_m in KW suggests more sustained, although strongly suppressed, biomass accumulation before growth was strongly suppressed. These results demonstrate

that logistic growth parameters provide additional biological insight beyond conventional biomass measurements by describing the temporal dynamics of growth limitation under salinity. Nevertheless, growth parameters were derived under hydroponic greenhouse conditions and may differ under field conditions.

Nutrient analysis of KW further demonstrated that severe salinity disrupted ionic homeostasis through excessive Na accumulation, depletion of K, Ca, and S, increased Na/K ratios, reduced K/Mg ratios, and decreased accumulation of several essential micronutrients. These responses are consistent with Na^+ competition for K^+ uptake and the resulting disruption of cation balance commonly reported in salt-stressed rice and other crops (Akter & Oue, 2018; Deinlein et al., 2014; Munns & Tester, 2008; Parisa et al., 2025; Wakeel, 2013). Reduced nutrient accumulation likely resulted from both impaired nutrient uptake and the substantial reduction in plant biomass under severe salinity. Because nutrient profiling was conducted only in KW, cultivar differences in nutrient homeostasis could not be evaluated and warrant future investigation. Together, these findings indicate that physiological stability during salt exposure and recovery capacity after stress release represent complementary components of salinity resilience in rice.

4. Conclusions

Stepwise salinity stress significantly reduced growth, biomass accumulation, water status, membrane stability, and chlorophyll content in both KW and RD6 rice cultivars. Logistic growth analysis demonstrated severe suppression of biomass accumulation, reflected by marked reductions in predicted asymptotic dry mass and maximum growth rate under salt stress. RD6 maintained higher RWC, CMS, and chlorophyll contents during salt exposure, indicating greater physiological stability. In contrast, KW exhibited stronger recovery of biomass and chlorophyll following salt removal despite greater physiological disruption during stress. Nutrient analysis in KW further revealed severe ionic imbalance characterized by excessive Na accumulation, depletion of essential nutrients, increased Na/K ratio, and reduced K/Mg ratio. Collectively, these findings indicate that RD6 maintained physiological function more effectively during salt exposure, whereas KW exhibited superior post-stress recovery. Integrating morpho-physiological traits, logistic growth analysis, and nutrient profiling provides useful insights into salinity responses and post-stress recovery in glutinous rice. However, the present findings were obtained under controlled hydroponic greenhouse conditions using only two rice cultivars, with nutrient profiling conducted only in KW under a single severe salinity regime. Furthermore, the high NaCl concentrations applied in this study may not fully represent field conditions; therefore, future studies should validate these responses across a wider range of rice genotypes and under more representative field environments.

5. Acknowledgements

The authors gratefully acknowledge the Faculty of Agricultural Technology, Kalasin University, for providing greenhouse and laboratory for this study.

6. Authors' Contributions

Prasit Khunsanit: designed research; performed research; wrote the paper.
Phichaiphusit Bubparn,Tanaphoom Boonmee and Nattapon Kan-a-roon: performed research.

Urai Kollboon and Keeravit Petjul: coordinated research.

ORCID
Prasit Khunsanit https://orcid.org/0009-0005-5081-1439
Tanaphooom Boonmee https://orcid.org/0009-0003-0756-4810
Nattapon kan-a-roon https://orcid.org/0009-0007-3072-7680
Urai Kollboon https://orcid.org/0009-0008-7129-3855
Keeravit Petjul https://orcid.org/0009-0007-3972-0231

7. Conflicts of Interest

The authors declare that they have no conflicts of interest.

References

Akter, M., & Oue, H. (2018). Effect of saline irrigation on accumulation of Na+, K+, Ca2+, and Mg2+ ions in rice plants. *Agriculture*, *8*(10), Article 164. https://doi.org/10.3390/agriculture8100164

Arunin, S., & Pongwichian, P. (2015). Salt-affected soils and management in Thailand. *Bulletin of the Society of Sea Water Science, Japan*, *69*(5), 319-325. https://doi.org/10.11457/swsj.69.319

Balansag, G. V. A., Anud, E. M. Jr., Balansag, G. P. A., Anud, K. M., & Balansag, G. N. A. (2023). The effect of AB mix nutrient solution on the height, number of leaves and fresh weight of lettuce (*Lactuca sativa* L.) in hydroponics cultivation system. *International Journal of Applied Science and Research*, *6*(2), 93-100. https://doi.org/10.56293/IJASR.2022.5510

Balasubramaniam, T., Shen, G., Esmaeili, N., & Zhang, H. (2023). Plants' response mechanisms to salinity stress. *Plants*, *12*(12), Article 2253. https://doi.org/10.3390/plants12122253

Barman, M., Pramanik, K., Chanda, R., Dash, S. S. S., Kundu, R., Roy, S., Pati, S., Pati, B., Banerjee, H., & Das, A. (2025). Unravelling salt tolerance in rice through multiphase evaluation integrating morpho-physiological, biochemical and molecular insights. *Plant Stress*, *18*, Article 101086. https://doi.org/10.1016/j.stress.2025.101086

Benjamini, Y., & Hochberg, Y. (1995). Controlling the false discovery rate: A practical and powerful approach to multiple testing. *Journal of the Royal Statistical Society: Series B (Methodological)*, *57*(1), 289-300.

Deinlein, U., Stephan, A. B., Horie, T., Luo, W., Xu, G., & Schroeder, J. I. (2014). Plant salt-tolerance mechanisms. *Trends in Plant Science*, *19*(6), 371-379. https://doi.org/10.1016/j.tplants.2014.02.001

Fisher, R. A. (1915). Frequency distribution of the values of the correlation coefficient in samples from an indefinitely large population. *Biometrika*, *10*(4), 507-521.

Gregoria, G. B., Senadhira, D., & Mendoza, R. D. (1997). *Screening rice for salinity tolerance*. IRRI.

Hsieh, C.-Y., Chen, H., Wu, Y.-C., Teng, C.-Y., & Li, C.-H. (2026). Using critical points of logistic model to describe the growth of rice plant height in Taiwan. *Scientific Reports, 16*, Article 10081. https://doi.org/10.1038/s41598-026-41295-8

Hsieh, C.-Y., Fang, S.-L., Wu, Y.-F., Chu, Y.-C., & Kuo, B.-J. (2021). Using sigmoid growth curves to establish growth models of tomato and eggplant stems suitable for grafting in subtropical countries. *Horticulturae*, *7*(12), Article 537. https://doi.org/10.3390/horticulturae7120537

Hunt, R. (1982). *Plant growth curves: The functional approach to plant growth analysis*. Edward Arnold.

Kojonna, T., Suttiyut, T., Khunpolwattana, N., Pongpanich, M., Suriya-Arunroj, D., Comai, L., Buaboocha, T., & Chadchawan, S. (2022). Identification of a negative regulator for salt tolerance at seedling stage via a genome-wide association study of Thai rice populations. *International Journal of Molecular Sciences*, *23*(3), Article 1842. https://doi.org/10.3390/ijms23031842

Liu, C., Mao, B., Yuan, D., Chu, C., & Duan, M. (2022). Salt tolerance in rice: Physiological responses and molecular mechanisms. *The Crop Journal*, *10*(1), 13-25. https://doi.org/10.1016/j.cj.2021.02.010

Moran, R. (1982). Formulae for determination of chlorophyllous pigments extracted with N, N-dimethylformamide. *Plant Physiology*, *69*(6), 1376-1381. https://doi.org/10.1104/pp.69.6.1376

Munns, R., Day, D. A., Fricke, W., Watt, M., Arsova, B., Barkla, B. J., Bose, J., Byrt, C. S., Chen, Z. H., & Foster, K. J. (2020). Energy costs of salt tolerance in crop plants. *New Phytologist*, *225*(3), 1072-1090. https://doi.org/10.1111/nph.15864

Munns, R., & Tester, M. (2008). Mechanisms of salinity tolerance. *Annual Review of Plant Biology*, *59*, 651-681. https://doi.org/10.1146/annurev.arplant.59.032607.092911

Parisa, D., Sagervanshi, A., Abdalla, M. A., & Mühling, K.-H. (2025). Na^{+}/Mg^{2+} ratio: a new physiological trait for salt resistance in faba bean (*Vicia faba* L.). *BMC Plant Biology*, *25*(1), Article 1568. https://doi.org/10.1186/s12870-025-07698-x

Poovarodom, S. (2009). *Growth and nutrient uptake into mangosteen (Garcinia mangostana L.) fruit.* https://escholarship.org/uc/item/5rk9h6k2

Posit Team. (2026). *RStudio: Integrated development environment for R*. Posit Software. http://www.posit.co/

R Core Team. (2023). *R: a language and environment for statistical computing*. R *Foundation for Statistical Computing*

Sackey, O. K., Feng, N., Mohammed, Y. Z., Dzou, C. F., Zheng, D., Zhao, L., & Shen, X. (2025). A comprehensive review on rice responses and tolerance to salt stress. *Frontiers in Plant Science*, *16*, Article 1561280. https://doi.org/10.3389/fpls.2025.1561280

Saleem, M. A., Khan, A., Tu, J., Huang, W., Liu, Y., Feng, N., Zheng, D., & Xue, Y. (2025). Salinity stress in rice: multilayered approaches for sustainable tolerance. *International Journal of Molecular Sciences*, *26*(13), Article 6025. https://doi.org/10.3390/ijms26136025

Santanoo, S., Khianpho, O., Sanitchon, J., & Theerakulpisut, P. (2025). Physiological and growth responses of Thai rice genotypes to high salinity stress at the seedling and reproductive stages. *Plants*, *14*(24), Article 3748. https://doi.org/10.3390/plants14243748

Siddique, M. A., Egdane, J., Bagunu, E., Quick, W. P., Diaz, M. G. Q., & Henry, A. (2025). Optimizing a protocol for salinity recovery during seedling stage in rice. *Plant Production Science*, *28*(4), 257-271.

Tarolli, P., Luo, J., Park, E., Barcaccia, G., & Masin, R. (2024). Soil salinization in agriculture: Mitigation and adaptation strategies combining nature-based solutions and bioengineering. *Iscience*, *27*(2), Article 108830. https://doi.org/10.1016/j.isci.2024.108830

Thornley, J. H., & Johnson, I. R. (1990). *Plant and crop modelling*. Clarendon Oxford.

Vanavichit, A., Kamolsukyeunyong, W., Siangliw, M., Siangliw, J. L., Traprab, S., Ruengphayak, S., Chaichoompu, E., Saensuk, C., Phuvanartnarubal, E., Toojinda, T. & Tragoonrung, S. (2018). Thai Hom Mali Rice: Origin and breeding for subsistence rainfed lowland rice system. *Rice*, *11*, Article 20. https://doi.org/ 10.1186/s12284-018-0212-7

Wakeel, A. (2013). Potassium–sodium interactions in soil and plant under saline-sodic conditions. *Journal of Plant Nutrition and Soil Science*, *176*(3), 344-354. https://doi.org/10.1002/jpln.201200417

Wickham, H. (2009). *ggplot2: Elegant graphics for data analysis*. Springer.
Xu, Y., Bu, W., Xu, Y., Fei, H., Zhu, Y., Ahmad, I., Nimir, N. E. A., Zhou, G., & Zhu, G. (2024). Effects of salt stress on physiological and agronomic traits of rice genotypes with contrasting salt tolerance. *Plants*, *13*(8), Article 1157. https://doi.org/10.3390/plants13081157